



A new approach for turn-on fluorescence sensing of L-DOPA†

Lu Wang,[‡] Dongdong Su,[‡] Stuart N. Berry,^{ab} Jungyeol Lee^c and Young-Tae Chang^{‡*acd}

Cite this: *Chem. Commun.*, 2017, 53, 12465

Received 1st October 2017,
 Accepted 27th October 2017

DOI: 10.1039/c7cc07640a

rsc.li/chemcomm

A novel design strategy for the fluorescence sensing of L-DOPA is reported. Resa-Sulf displays a significant turn-on fluorescence response to L-DOPA due to its reduction properties; this sensing mechanism was fully confirmed by mechanistic studies. Furthermore, Resa-Sulf was successfully utilized to quantitatively detect L-DOPA concentrations from a commercially available source.

Dopamine is known as an important neurotransmitter of the human central nervous system and affects many brain functions and behavioral responses.^{1,2} Lack of dopamine in the brain may lead to neurological disorders, such as schizophrenia and Parkinson's disease. The precursor to dopamine, L-DOPA is converted to dopamine *via* a metabolic pathway and, unlike dopamine, L-DOPA has the ability to cross the protective blood-brain barrier. This has allowed the external use of L-DOPA therapeutically to increase dopamine concentrations in the brain. Indeed, L-DOPA is successfully utilized as a drug in the treatment of Parkinson's disease and dopamine-responsive dystonia.³⁻⁵ Considering the biochemical significance of L-DOPA and its applications in the field of medicine, it is highly desirable to develop an efficient method for the quantitative detection of L-DOPA. Most reported methods for L-DOPA detection have mainly been restricted to the electrochemical study through the use of electrodes composed of nanorods, nanotubes or graphene nanohybrids.⁶⁻⁹ Compared to other analytical technology, fluorescent molecular sensors are more attractive, due to their high sensitivity and ease of visibility.^{10,11}

Up to now, only limited numbers of small molecule fluorescent sensors for L-DOPA have been reported.¹²⁻¹⁴ Furthermore, most of these small molecule sensors rely on quenching or turn-off sensing mechanisms. It is known that turn-on sensors have comparatively better sensitivity, higher resolution as well as lower potential errors than turn-off sensors. A good turn-on sensor, therefore, may have unique potential for the future real-time *in vivo* or *ex vivo* imaging of L-DOPA.

Herein, we have demonstrated a new approach for turn-on fluorescence sensing of L-DOPA by using its reduction properties. The tendency of L-DOPA to donate an electron in solution can be exploited by using it as a reductant in a redox reaction and based on this, we sought to develop a redox reaction based turn-on fluorescence sensor for L-DOPA.^{15,16} The major advantage of redox reaction sensing is that the molecular recognition events can occur in a short time span, with observable changes in color and/or fluorescence intensity. Furthermore, quantitative detection can be easily achieved because of the stoichiometric nature of the redox reaction. Up to now, according to the selected redox reaction system, several examples based on redox reactions have been developed for appropriate applications.¹⁷⁻²⁰

Catecholamines with reduction properties can be oxidized in either water or buffer solution. This property has been previously applied in methods based on the electrochemical analysis of dopamine.²¹⁻²³ Inspired by this detection approach, we report a novel design strategy for the preparation of fluorescent sensors for the detection of L-DOPA. To the best of our knowledge, this is the first fluorescent sensor for L-DOPA based on a redox reaction. To demonstrate the application of this redox reactive approach, we employed a resazurin dye as our signal reporter not only due to its sensitive and simple mechanism of action, but also due to its unique oxidative and electron dependent optical properties.²⁴ Our previous work has also shown that resazurin-based dyes can be utilized in redox reaction based sensors.²⁵

Scheme 1 indicates the structures of the fluorescent sensors investigated in this study and the proposed sensing approach. Resazurin-based sensors (**Resa-Sulf** and **Resa-Con**) are shown as self-quenching fluorophores, however, upon addition of L-DOPA,

^a Laboratory of Bioimaging Probe Development, Singapore Bioimaging Consortium (SBIC), Agency for Science, Technology and Research (A*STAR), 11 Biopolis Way, 02-02 Helios, Biopolis, Singapore 138667, Singapore

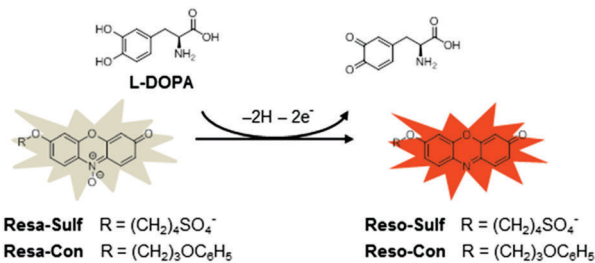
^b Chemistry, University of Southampton, Southampton, SO17 1BJ, UK

^c Department of Chemistry, Pohang University of Science and Technology, 77 Cheongam-Ro, Nam-Gu, Pohang 37673, Republic of Korea.
 E-mail: ytchang@postech.ac.kr

^d Center for Self-Assembly and Complexity, Institute for Basic Science (IBS), Pohang 37673, Republic of Korea

† Electronic supplementary information (ESI) available: Procedures for the synthesis and characterization of the sensors used in this study and additional spectroscopic information. See DOI: 10.1039/c7cc07640a

‡ These authors contributed equally.



Scheme 1 The structures of fluorescent sensors and the proposed sensing mechanism of L-DOPA.

a redox reaction occurs and L-DOPA as the reductant reduces the weakly fluorescent resazurin fluorophore, leading to deoxygenation of the N-oxide group, producing the resultant resorufin structures as strongly fluorescent products. The synthesis of these sensors is described in Fig. S1 (ESI[†]), and all sensors were fully characterized by ¹H NMR, ¹³C NMR and HRMS (shown in the ESI[†]).

To obtain the optimum sensing conditions, the fluorescence response of Resa-Con to different analytes as functions of time and pH was systematically studied in DMSO/PBS buffer solution (v/v = 1:1). As shown in Fig. S2 (ESI[†]), Resa-Con is almost non-fluorescent over a large pH range from 4.3 to 11.2. Upon treatment with L-DOPA, as well as other catecholamines, the fluorescence is enhanced. Furthermore, the fluorescence enhancement is greater in weakly basic solutions compared to under acidic conditions. By evaluating the reaction rate, upon addition of analytes at pH 11.2, the fluorescence is almost saturated within 3 min of analyte addition, and a color change from red to yellow is observed. This makes it possible to detect L-DOPA *via* the naked eye or under irradiation using a UV lamp. These results are consistent with a previous study which shows that the absorption and fluorescence properties of resazurin and resorufin are dependent on pH, and that the fluorescence is enhanced at higher pH.¹⁹ Unfortunately, under these conditions, Resa-Con does not show perfect selectivity towards other catecholamines, such as dopamine, epinephrine and norepinephrine. This result is not surprising, because these three types of catecholamines share similar functional groups.^{26–28}

In order to reduce the fraction of DMSO in the sensing system, we prepared Resa-Sulf to improve aqueous solubility. By comparing the fluorescence responses of Resa-Con and Resa-Sulf towards L-DOPA, we found that with 50% DMSO as a co-solvent, the maximum fluorescence intensities of the two sensors were essentially the same in the presence of L-DOPA; however, in 1% DMSO/PBS buffer, the highest fluorescence intensity of the water-soluble fluorescent sensor, Resa-Sulf, is almost 7 times that of non-water-soluble Resa-Con after 2 min of incubation. This provides higher sensitivity and a larger response range in the aqueous environment (Fig. S3, ESI[†]). Clearly, aggregation of Resa-Con was observed in 1% DMSO/PBS buffer (Fig. S4, ESI[†]). Considering the fast response and high sensitivity between Resa-Sulf and L-DOPA, 1% DMSO/PBS buffer at pH 11.2 was selected as the sensing solvent for further experiments. Subsequently, the time-dependent fluorescence changes of Resa-Sulf (50 μM) in the presence of L-DOPA (0–100 μM) were investigated. This experiment

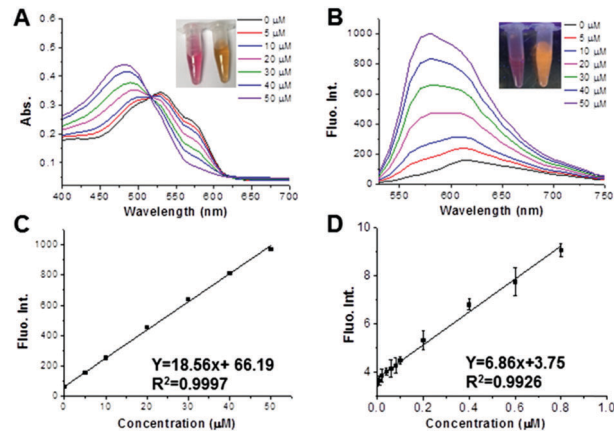


Fig. 1 (A) UV-Vis absorption and (B) fluorescence spectra of Resa-Sulf (50 μM) during the titration with increasing concentrations of L-DOPA (0–50 μM). Inset: (A) The color and (B) fluorescence images of Resa-Sulf (50 μM) in the absence and presence of L-DOPA (50 μM). Incubation time: 2 min. (C) Plot of the fluorescence intensity of Resa-Sulf (50 μM) at 570 nm against the concentrations of L-DOPA from 0 to 50 μM. Incubation time: 2 min. (D) Plot of the fluorescence intensity of Resa-Sulf (1 μM) at 570 nm against the concentrations of L-DOPA from 0 to 0.8 μM. Incubation time: 2 min. $\lambda_{\text{ex}} = 480$ nm, 25 °C.

showed that the enhanced fluorescence intensity saturates within nearly 2 minutes of incubation (Fig. S5, ESI[†]).

Encouraged by the fast response, we then tested the reactivity of Resa-Sulf upon addition of L-DOPA in PBS with an incubation time of 2 min. The spectral changes of Resa-Sulf during the titration with L-DOPA are shown in Fig. 1. Upon addition of increasing concentrations of L-DOPA, the maximum absorption band changed from 530 nm to 480 nm, meanwhile, the fluorescence band centered at 615 nm blue-shifts to 580 nm, which results from the redox reaction between Resa-Sulf and L-DOPA (movie, ESI[†]). Pleasingly, the changes in fluorescence intensities of Resa-Sulf (50 μM) showed a linear calibration response to L-DOPA concentrations from 0 to 50 μM with the coefficient of determination $R^2 = 0.9997$ (Fig. 1C). Furthermore, to test the sensitivity of Resa-Sulf, similar fluorescence titrations were performed with Resa-Sulf at 1 μM, and the fluorescence response to L-DOPA also showed a good linear relationship ($R^2 = 0.9926$) even at very low L-DOPA concentrations ranging from 0 to 0.8 μM (Fig. 1D). Notably, the detectable concentration of L-DOPA can be as low as 0.01 μM. More importantly, as one of the advantages of redox reaction based sensing, the ratio of the sensor to analyte can be easily identified based on the nature of the redox reaction. As expected, the fluorescence of Resa-Sulf (20 μM) increased to the maximum level at a concentration of L-DOPA of 20 μM in 10 min, which suggests that the ratio between Resa-Sulf and L-DOPA is 1:1 (Fig. S6, ESI[†]). Furthermore, Job's plot analysis also confirmed a 1:1 reaction stoichiometry (Fig. S7, ESI[†]).²⁹ The fast response and the clear reaction ratio suggest that Resa-Sulf has good potential for application in the quantitative detection of L-DOPA concentrations.

In order to examine the selectivity of Resa-Sulf towards L-DOPA, the fluorescence changes of Resa-Sulf in the presence of different redox reagents, such as NADH, catechol and amino acids, were examined by monitoring the changes of the peak maxima at 570 nm. With the exception of dopamine, epinephrine

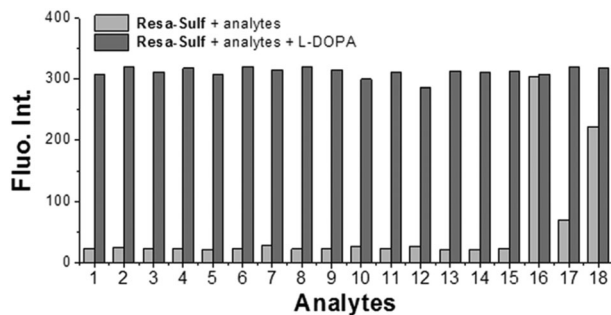


Fig. 2 Fluorescence responses of **Resa-Sulf** (20 μM) upon addition of various relevant redox reagents. Incubation time: 5 min; analytes (50 μM): (1) PBS buffer; (2) NADPH; (3) NADH; (4) NAD⁺; (5) ATP; (6) Met; (7) Cys; (8) Tyr; (9) phenol; (10) catechol; (11) glucose; (12) GSH; (13) Na⁺; (14) K⁺; (15) Cl⁻; (16) dopamine; (17) epinephrine; and (18) norepinephrine. The light gray bar represents the fluorescence intensity of only a single analyte with **Resa-Sulf**; the dark gray bar represents the fluorescence intensity of the analyte and L-DOPA with **Resa-Sulf**. $\lambda_{\text{ex}} = 480 \text{ nm}$, $\lambda_{\text{em}} = 570 \text{ nm}$, 25 $^{\circ}\text{C}$.

and norepinephrine, which share similar structures with L-DOPA, all other species showed no response to **Resa-Sulf**. Upon addition of an equivalent amount of L-DOPA to each competitive species, the fluorescence enhancement is recovered (Fig. 2). In particular, **Resa-Sulf** does not respond to catechol, probably due to the differences in the electrochemical properties to catecholamines. These results indicated that **Resa-Sulf** has relatively good selectivity for L-DOPA and catecholamines over other biologically relevant redox reagents. Therefore, **Resa-Sulf** shows potential application in L-DOPA analysis in the absence of catecholamines. It should be noted that only in the presence of dopamine is a similar fluorescence response observed: epinephrine and norepinephrine give small fluorescence maxima compared to in the presence of L-DOPA. The reaction rate constants are shown in Fig. S8 (ESI[†]). Considering the complexity of the intracellular environment, it is difficult to use this probe for neurotransmitter imaging by simple incubation; however, it still has high potential for cell imaging if the probe can be delivered into specific organelles in neuronal cells.³⁰

To obtain more detailed insights into the sensing mechanism, HPLC-MS was employed to characterize the reaction between **Resa-Sulf** and L-DOPA.³¹ The **Resa-Sulf** samples were injected for HPLC before and after 2 min of incubation of L-DOPA. The results from this HPLC-MS test showed that the signal corresponding to **Resa-Sulf** at 8.1 min disappeared and a new peak corresponding to the reduction product **Reso-Sulf** at 8.5 min emerged (Fig. 3). The results were further confirmed by mass spectral analysis. The signal at 8.1 min shows characteristic mass information for **Resa-Sulf**, while the new peak at 8.5 min shows mass information for the reduction product **Reso-Sulf** (Fig. S9, ESI[†]).

To further confirm the proposed sensing mechanism, the reaction of **Resa-Sulf** with L-DOPA was also analyzed by ¹H NMR spectroscopy. As shown in Fig. 4, upon the addition of L-DOPA, the major peaks of **Resa-Sulf** ranging from 6 ppm to 8 ppm disappeared, while new peaks corresponding to the **Reso-Sulf** product clearly emerged. In particular, the two doublets at 8.02 ppm and 7.98 ppm which correspond to the proton resonances on either side of the N-oxide group undergo a large upfield shift to 7.55 ppm and 7.38 ppm respectively in the reduced species due to the loss of

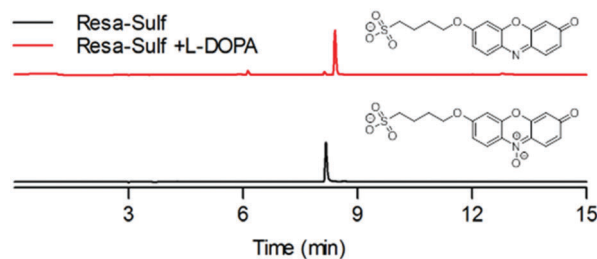


Fig. 3 HPLC-MS spectral changes observed for **Resa-Sulf** (100 μM) upon addition of L-DOPA (500 μM). The absorbance signals were collected at 500 nm.

deshielding effects. Furthermore, **Reso-Sulf** was successfully isolated and fully characterized in high yield after the reaction of **Resa-Sulf** with L-DOPA (see the ESI[†] for synthesis and characterization). Taken together, these results clearly confirm the reductive sensing mechanism of L-DOPA with **Resa-Sulf**.

Our goal is to develop a simple and reliable sensing method for the quantitative detection of L-DOPA in real samples. Many health care products containing L-DOPA are sold as mood enhancers or to improve stress responses, and also as drugs for the treatment of Parkinson's disease and dopamine-responsive dystonia; however, overuse of L-DOPA may cause serious side effects, such as nausea, vomiting, strong headaches, and disruption of sleep cycles.^{5,32} In order to quantitatively detect L-DOPA concentrations, we applied **Resa-Sulf** to analyse L-DOPA in real samples. Standard calibration curves were developed using fluorescence and HPLC methods with known, different concentrations of pure L-DOPA (Fig. S10 and S11, ESI[†]).³³ By comparing the actual L-DOPA amount acquired from HPLC and fluorescence measurements, we found that the calculated data for L-DOPA from different methods correlated very well, thus confirming that **Resa-Sulf** is feasible for practical determination of L-DOPA in real samples. A commercially available source, DOPA Mucuna Veg Capsules, was purchased from Now Foods and used without further treatment. The DOPA capsule was dissolved and diluted before analysis by treatment with **Resa-Sulf**. Table 1 shows that **Resa-Sulf** can be used to determine the concentration of L-DOPA in commercial

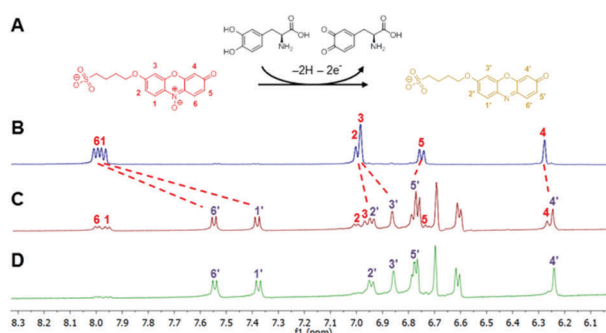


Fig. 4 Partial ¹H NMR spectra showing the reaction of **Resa-Sulf** (10 mM) and L-DOPA (20 mM) in D₂O. (A) The proposed sensing mechanism with proton assignment. (B) **Resa-Sulf** only. (C) **Resa-Sulf** and L-DOPA in the middle of the reaction. (D) **Resa-Sulf** and L-DOPA after completion of the reaction.

Table 1 L-DOPA amount acquired using the fluorescence and HPLC method

DOPA Mucuna Veg Capsules (15% L-DOPA)	Average concentration ^a (mM)	Calculated percentage (%)
Fluorescence method	0.877 ± 0.023	13.09 ± 0.34
HPLC method	0.861 ± 0.042	12.85 ± 0.62

^a Sample preparation: 9.9 mg sample was dissolved in 7.5 mL DI water (stock sample solution), strenuous vibration for 5 min, then filtered to remove insoluble substances. Fluorescence method: 4 µL stock sample solution was added to **Resa-Sulf** (50 µM, 196 µL, PBS buffer pH 11.2), incubation time: 2 min. HPLC Method: 50 µL stock sample solution was injected into HPLC for L-DOPA peak area calculation. Values are represented as means and error bars as standard deviations ($n = 3$).

samples with good recovery. The level of L-DOPA was calculated to be 13.09% and 12.85% based on **Resa-Sulf** and HPLC measurements respectively (Fig. S12, ESI[†]), which agrees well with the content declared by the company (15%). Thus, **Resa-Sulf** can be utilized as a simple tool to accurately quantify L-DOPA concentrations in commercially available health care products or L-DOPA containing plants.

In summary, by exploiting the reductive properties of L-DOPA, we have found a simple, rapid turn-on sensor for the quantitative detection of L-DOPA for the first time. The water-soluble sensor **Resa-Sulf** shows high selectivity and fast response towards L-DOPA, and the nature of the redox reaction makes it a good, practical tool for the quantitative detection of L-DOPA in real samples. This approach was successfully applied in the detection of a commercially available source of L-DOPA with a simple operation process. HPLC-MS and ¹H NMR studies provided a strong support for the mechanism of L-DOPA detection by **Resa-Sulf**. Therefore, this new approach not only provides an efficient tool for L-DOPA detection, but also offers a novel design strategy for the future development of other catecholamines sensors.

We gratefully acknowledge the intramural funding from A*STAR (Agency for Science, Technology and Research, Singapore) Biomedical Research Council and National Medical Research Council grant (NMRC/TCR/016-NNI/2016).

Conflicts of interest

There are no conflicts to declare.

Notes and references

- 1 P. C. Rodriguez, D. B. Pereira, A. Borgkvist, M. Y. Wong, C. Barnard, M. S. Sonders, H. Zhang, D. Sames and D. Sulzer, *Proc. Natl. Acad. Sci. U. S. A.*, 2013, **110**, 870–875.

- 2 V. M. Lopez, C. L. Decatur, W. D. Stamer, R. M. Lynch and B. S. McKay, *PLoS Biol.*, 2008, **6**, e236.
- 3 K. J. Broadley, *Pharmacol. Ther.*, 2010, **125**, 363–375.
- 4 K. Hyland and P. T. Clayton, *Clin. Chem.*, 1992, **38**, 2405–2410.
- 5 D. Merims and N. Giladi, *Parkinsonism Relat. Disord.*, 2008, **14**, 273–280.
- 6 E. Molaakbari, A. Mostafavi, H. Beitollahi and R. Alizadeh, *Analyst*, 2014, **139**, 4356–4364.
- 7 F. R. Leite, C. M. Maroneze, A. B. de Oliveira, W. T. dos Santos, F. S. Damos and C. Silva Luz Rde, *Bioelectrochemistry*, 2012, **86**, 22–29.
- 8 S. Ates, E. Zor, I. Akin, H. Bingol, S. Alpaydin and E. G. Akgemci, *Anal. Chim. Acta*, 2017, **970**, 30–37.
- 9 V. N. Palakollu, N. Thapliyal, T. E. Chiwunze, R. Karpoomath, S. Karunanidhi and S. Cherukupalli, *Mater. Sci. Eng., C*, 2017, **77**, 394–404.
- 10 X. Li, X. Gao, W. Shi and H. Ma, *Chem. Rev.*, 2014, **114**, 590–659.
- 11 M. S. Goncalves, *Chem. Rev.*, 2009, **109**, 190–212.
- 12 J. Yoon and A. W. Czarnik, *Bioorg. Med. Chem.*, 1993, **1**, 267–271.
- 13 A. Coskun and E. U. Akkaya, *Org. Lett.*, 2004, **6**, 3107–3109.
- 14 X. X. Chen, X. Wu, P. Zhang, M. Zhang, B. N. Song, Y. J. Huang, Z. Li and Y. B. Jiang, *Chem. Commun.*, 2015, **51**, 13630–13633.
- 15 T. Liu, L.-L. Han, C.-M. Du and Z.-Y. Yu, *Russ. J. Phys. Chem. A*, 2014, **88**, 1085–1090.
- 16 X. M. Shen, F. Zhang and G. Dryhurst, *Chem. Res. Toxicol.*, 1997, **10**, 147–155.
- 17 K. Tanabe, N. Hirata, H. Harada, M. Hiraoka and S. Nishimoto, *ChemBioChem*, 2008, **9**, 426–432.
- 18 Y. Yamada, Y. Tomiyama, A. Morita, M. Ikekita and S. Aoki, *Chem-BioChem*, 2008, **9**, 853–856.
- 19 E. Nakata, Y. Yukimachi, H. Kariyazono, S. Im, C. Abe, Y. Uto, H. Maezawa, T. Hashimoto, Y. Okamoto and H. Hori, *Bioorg. Med. Chem.*, 2009, **17**, 6952–6958.
- 20 S. Takahashi, W. Piao, Y. Matsumura, T. Komatsu, T. Ueno, T. Terai, T. Kamachi, M. Kohno, T. Nagano and K. Hanaoka, *J. Am. Chem. Soc.*, 2012, **134**, 19588–19591.
- 21 S. Govindaraju, S. R. Ankireddy, B. Viswanath, J. Kim and K. Yun, *Sci. Rep.*, 2017, **7**, 40298.
- 22 Q. Mu, H. Xu, Y. Li, S. Ma and X. Zhong, *Analyst*, 2014, **139**, 93–98.
- 23 H. Huang, Y. Gao, F. Shi, G. Wang, S. M. Shah and X. Su, *Analyst*, 2012, **137**, 1481–1486.
- 24 C. Bueno, M. L. Villegas, S. G. Bertolotti, C. M. Previtali, M. G. Neumann and M. V. Encinas, *Photochem. Photobiol.*, 2002, **76**, 385–390.
- 25 L. Wang, J. Zhang, B. Kim, J. Peng, S. N. Berry, Y. Ni, D. Su, J. Lee, L. Yuan and Y. T. Chang, *J. Am. Chem. Soc.*, 2016, **138**, 10394–10397.
- 26 M. Maue and T. Schrader, *Angew. Chem., Int. Ed.*, 2005, **44**, 2265–2270.
- 27 K. E. Secor and T. E. Glass, *Org. Lett.*, 2004, **6**, 3727–3730.
- 28 K. S. Hettie and T. E. Glass, *Chem. – Eur. J.*, 2014, **20**, 17488–17499.
- 29 J. S. Renny, L. L. Tomasevich, E. H. Tallmadge and D. B. Collum, *Angew. Chem., Int. Ed.*, 2013, **52**, 11998–12013.
- 30 H. Fang, M. L. Pajski, A. E. Ross and B. J. Venton, *Anal. Methods*, 2013, **5**, 2704–2711.
- 31 D. Su, C. L. Teoh, S. Sahu, R. K. Das and Y. T. Chang, *Biomaterials*, 2014, **35**, 6078–6085.
- 32 M. H. Brilliant, K. Vaziri, T. B. Connor, Jr., S. G. Schwartz, J. J. Carroll, C. A. McCarty, S. J. Schrodi, S. J. Hebring, K. S. Kishor, H. W. Flynn, Jr., A. A. Moshfeghi, D. M. Moshfeghi, M. E. Fini and B. S. McKay, *Am. J. Med.*, 2016, **129**, 292–298.
- 33 W. Xu, T.-H. Kim, D. Zhai, J. C. Er, L. Zhang, A. A. Kale, B. K. Agrawalla, Y.-K. Cho and Y.-T. Chang, *Sci. Rep.*, 2013, **3**, 2255.